Carbohydrate Polymers 87 (2012) 518–523

Contents lists available at ScienceDirect

Carbohydrate Polymers

journal homepage: www.elsevier.com/locate/carbpol

Asymmetrical flow field-flow fractionation enables the characterization of molecular and supramolecular properties of cereal β-glucan dispersions

Andreas Håkansson[a], Matilda Ulmius[b], Lars Nilsson[a,*]

[a] Department of Food Technology, Engineering and Nutrition, Faculty of Engineering LTH, Lund University, P.O. Box 124, SE-221 00 Lund, Sweden
[b] Biomedical Nutrition, Pure and Applied Biochemistry, Faculty of Engineering LTH, Lund University, P.O. Box 124, SE-221 00 Lund, Sweden

ARTICLE INFO

Article history:
Received 12 July 2011
Received in revised form 29 July 2011
Accepted 4 August 2011
Available online 11 August 2011

Keywords:
Beta-glucan
Asymmetrical flow field-flow fractionation
AF4
Oat
Barley

ABSTRACT

In this paper we study the properties of molecular and supra molecular species in cereal β-glucan solutions/dispersions by the utilization of asymmetrical flow field-flow fractionation coupled to multi-angle light scattering and refractive index (AsFlFFF-MALS-RI) detectors. The samples were purified barley and oat β-glucans which were dissolved in aqueous solution using either mild conditions or more harsh treatments with alkali. Dissolution in 0.5 M NaOH was not sufficient to eliminate aggregated structures in barley β-glucan. The results in this paper show how distinction can possibly be made between molecular and supra molecular species using scaling approaches and conformational parameters obtained from AsFlFFF-MALS-RI over the entire size distribution. Small species in the barley β-glucan samples display properties ranging from elongated conformation to random coil conformation. Aggregates have low apparent densities and a swollen micro gel structure. Oat β-glucan displays no properties that can be attributed to a molecularly dissolved β-glucan showing that dissolution was incomplete. The aggregate properties analyzed were similar between oat and barley β-glucan.

1. Introduction

The soluble fiber β-glucan from oats and barley is accepted by the US Food and Drug Administration as a functional, bioactive food ingredient, allowing a health claim that correlates the intake of the soluble fiber with reduced risk of coronary heart disease (US Food and Drug Administration, 1997, 2008). Also the scientific panel of the EU has reacted favorably to health claims associating β-glucan intake with maintained as well as lowered blood cholesterol levels (European Food Safety Authority, 2009, 2010). Cereal β-glucans are linear polysaccharides of β-D-glucopyranosyl units linked via a mixture of β-(1 → 3) and β-(1 → 4) linkages. The β-(1 → 4) linkages occur in groups of two or three, forming trimers and tetramers, but longer cellulose segments can also be found, separated by a β-(1 → 3) linkage. β-Glucans in oat and barley differ in their structural properties, such as the molar mass (oat > barley (Beer, Wood, & Weisz, 1997)) and the ratio of tri/tetramers (barley > oat (Cui, Wood, Blackwell, & Nikiforuk, 2000)). The functional properties are related to its solution behaviour, i.e. the ability of β-glucans to form viscous solutions. The viscosity, in turn, depends on the molar mass, concentration, solubility and the ability to form aggregates (Gómez, Navarro, Gamier, Horta, & Carbonell, 1997), and is promoted by the higher molar mass and the lower tri/tetramer ratio found in oats (less regular structure increases the solubility).

The aggregation of β-glucans, that also may be important for the viscosity increasing effects, have previously been detected using batch light scattering (Grimm, Krüger, & Burchard, 1995; Li, Cui, Wang, & Yada, 2011) or by confocal scanning laser microscopy (Kivelä, Nyström, Salovaara, & Sontag-Strohm, 2009; Wu et al., 2006). Such studies have suggested different aggregate structures, such as a fringed micelle structure (Grimm et al., 1995) or an opened irregular structure (Li et al., 2011), as well as different formation rates of the aggregation. In a recent study, we demonstrated that the major part of a barley β-glucan sample appeared aggregated when dissolved in water, using asymmetrical flow field-flow fractionation (AsFlFFF) connected to multi-angle light scattering (MALS) and refractive index (RI) detectors (Ulmius et al., 2012). This method is highly suitable for fractionation of polydisperse β-glucan samples. The present study reports on the continuing analysis of oat and barley β-glucan in aqueous environments using AsFlFFF. The purpose is to retain possible aggregates in order to obtain structural and conformational information on both molecular species as well as aggregates. Furthermore, we are investigating the effect of NaOH on the dissolution of β-glucans as well as the elution behaviour, in AsFlFFF, of the highly charged β-glucans under alkaline conditions. Dissolution in NaOH has been previously shown to disrupt/dissolve aggregates of β-glucans (Li et al., 2011; Li, Wang, Cui, Huang, & Kakuda, 2006).

* Corresponding author. Tel.: +46 46 222 8303; fax: +46 46 222 4622.
E-mail address: lars.nilsson@food.lth.se (L. Nilsson).

0144-8617/$ – see front matter © 2011 Elsevier Ltd. All rights reserved.
doi:10.1016/j.carbpol.2011.08.014

2. Experimental

2.1. β-Glucan

Oat β-glucan ("High viscosity" > 97% pure) and barley β-glucan ("Molar mass standards" > 95% pure) were purchased from Megazyme International Ltd., Bray, Ireland. The weight-average molar mass (M_w) for the barely β-glucan was specified as 3.59×10^5 g/mol which, according to the supplier, had been determined using high-performance size-exclusion chromatography (HPSEC) in 0.05 M NaOH, where the samples were dissolved by 10 min boiling prior to the analysis. Sample solutions with β-glucan, 0.25% (w/v), were prepared in pure water, 0.05 M NaOH or 0.5 M NaOH. Preparation of β-glucan samples in pure water was performed with magnetic stirring at 70 °C for 20 min while dissolution in NaOH was performed through stirring at room temperature for 30 min.

2.2. FFF analysis equipment

The AsFlFFF instrument was an Eclipse 3+ Separation System (Wyatt Technology Europe, Dernbach, Germany). It was connected to a Dawn Heleos II multi-angle light scattering (MALS) detector (Wyatt Technology) operating at a wavelength of 658 nm, an Optilab T-rEX differential refractive index (dRI) detector (Wyatt Technology) operating at a wavelength of 658 nm. An Agilent 1100 series isocratic pump (Agilent Technologies, Waldbronn, Germany) with an in-line vacuum degasser and an Agilent 1100 series autosampler delivered the carrier flow and handled sample injection onto the AsFlFFF channel. Between the pump and the channel was placed a filter-holder with a 100 nm pore-size polyvinylidene fluoride membrane (Millipore Corp.) to ensure that particle free carrier entered the channel. The AsFlFFF channel was a Wyatt long channel (Wyatt Technology) having a tip-to-tip length of 26.5 cm and a nominal thickness of 190 μm. The actual thickness was determined to be 182 μm by calibration against BSA in a similar manner to the procedure described in literature (Litzen, 1993). The ultrafiltration membrane forming the accumulation wall was made of polyethersulphone with a cut-off of 10 kDa (Microdyn-Nadir GmbH, Wiesbaden, Germany).

2.3. FFF separation parameters and data processing

The sample injection onto the channel was performed at a flow rate of 0.20 mL min^{-1} during 2.5 min. The sample volume injected onto the channel was 50–150 μL for an injected sample mass of approximately 125–150 μg. The injected amount was optimized in order to ensure no overloading in the channel by confirming that retention times were independent of the injected amount. A 4.5 min focusing/relaxation step was performed prior to elution with the focusing flow rate being identical to the initial cross-flow rate during elution (0.5 mL min^{-1}). In order to avoid excessive retention and long elution times a cross-flow rate which either decays exponentially with time (half-life = 4 min) or linearly (0.086 mL min^{-2}) was used as shown in Fig. 1. After elution the channel was flushed without any cross-flow for 5 min before the next analysis. Detector flow rate (V_{out}) was constant at 1.0 mL min^{-1} throughout the separation. Carrier liquids were either prepared as 10 mM $NaNO_3$ (Merck, Darmstadt, Germany) and 0.02% (w/v) NaN_3 (BDH, Poole, UK) or with 0.05 M or 0.5 M NaOH (Merck) dissolved in pure water prepared with a Milli-Q system (Millipore Corp.).

Processing of light scattering data was made by the Astra software, version 5.3.4.14 (Wyatt Technology). The molar mass and the r_{rms} were obtained by the Berry method (Andersson, Wittgren, & Wahlund, 2003; Berry, 1966) performing a first order fit to data obtained at 44.0–90.0° scattering angle. The lowest scattering angles, 32.0° and 38.0°, was not included, as the data obtained was imprecise. A dn/dc value of 0.146 mL g^{-1} was used and the second virial coefficient was assumed to be negligible. Differential distributions where obtained from fitting of the relevant data with a 4th degree exponential with the Astra software.

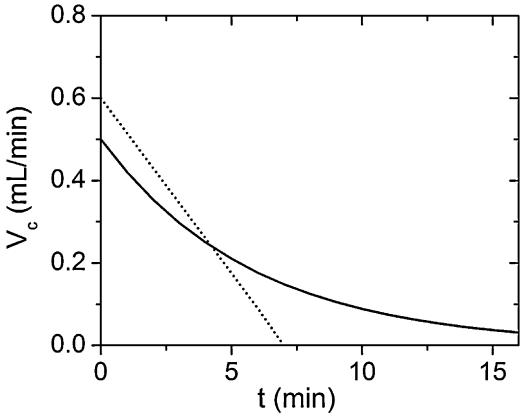

Fig. 1. Cross-flow (V_c) vs elution time (t) as used in the AsFlFFF experiments.

The hydrodynamic radius (r_h) was obtained from the Stokes–Einstein equation (Einstein, 1905)

$$r_{h,i} = \frac{k_b T}{6\pi\eta D_i} \tag{1}$$

where k_b is the Boltzmann constant, T is the temperature, η is the dynamic viscosity of the solvent and D_i is the diffusion coefficient. In turn, the diffusion coefficient was obtained from

$$\frac{dz_i}{dt} = f(V_c)D_i \tag{2}$$

where z_i is the position of sample component i along the channel, t is the time, k is a constant including flow conditions and geometrical parameters and V_c is the cross-flow rate. Eq. (2) is a highly condensed version of the full differential equation of which the derivation of and solution procedure was reported in an earlier paper (Nilsson, Leeman, Wahlund, & Bergenståhl, 2006).

The apparent densities were obtained from the molar mass and r_{rms} distributions assuming homogeneous distribution of mass and a spherical shape. As r_{rms} gives only an approximate description of the volume of possible shapes the density obtained should be considered as an apparent property. The apparent density, ρ_i, for component i of the sample is calculated from

$$\rho_i = \frac{M_i}{V(r_{rms})_i} \cdot q \tag{3}$$

where M is the molar mass, $V(r)$ is the volume of a sphere with radius r and q is given by Eq. (4).

$$q = \frac{V_{sphere}(r_{rms})}{V_{sphere}(r)} = \frac{r_{rms}^3}{r^3} = \frac{\left(\sqrt{3/5}\cdot r\right)^3}{r^3} = \left(\frac{3}{5}\right)^{3/2} \tag{4}$$

The mass-weighted average apparent density was obtained from

$$\bar{\rho} = \frac{\sum m_i \cdot \rho_i}{\sum m_i} \tag{5}$$

where m_i is the mass flow in each class i.

3. Results

The solution behaviour of β-glucan from oat and barley is investigated using mild dissolution conditions (water, stirring at 70 °C for

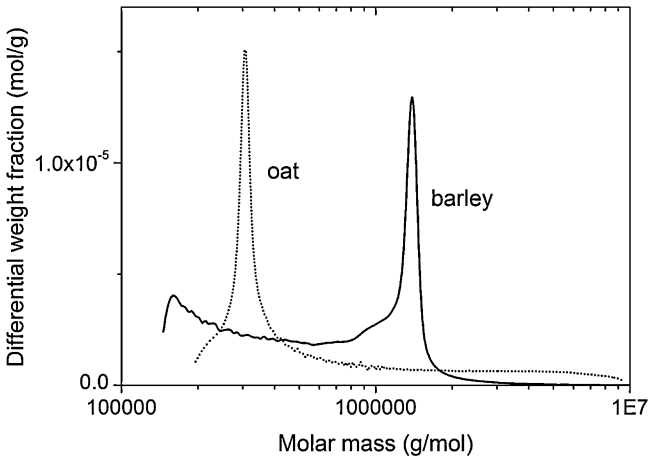

Fig. 2. Differential molar mass distribution for barley β-glucan (solid line) and oat β-glucan (dotted line).

20 min) or dissolution in alkali (0.05 M or 0.5 M NaOH, stirring at room temperature for 30 min).

The differential molar mass (M) distributions for the oat and barley β-glucan samples after dissolution in water with heating are shown in Fig. 2. The results show that oat β-glucan displays one distinct population peaking around 3.0×10^5 g/mol while the molar mass distribution tails up to about 1×10^7 g/mol, i.e. low amounts of high molar mass species. For barley β-glucan two distinct molar mass populations can be observed; one minor population peaking around 1.7×10^5 g/mol and the second peaking at about 1.5×10^6 g/mol.

Fig. 3 displays the root mean square radius (r_{rms}) distributions for oat and barley β-glucan respectively. In the case of barley β-glucan two distinct populations can be observed while the oat β-glucan has a considerably wider distribution, again tailing up to large sizes.

Conformational data for the two β-glucans are shown in Figs. 4 and 5 as apparent density and the ratio between r_{rms} and hydrodynamic radius (r_h) vs. M. In Fig. 5, M is replaced by the degree of aggregation ($M/M_{w,0}$) obtained from normalization of the measured M with the weight-average molar mass of the barley β-glucan single molecule ($M_{w,0}$) provided by the supplier (3.59×10^5 g/mol). In the case of oat-β glucan (Fig. 4) the apparent density initially decreases with increasing M and the levels off at a rather constant level, approximately at $M = 6 \times 10^6$ g/mol. The plot

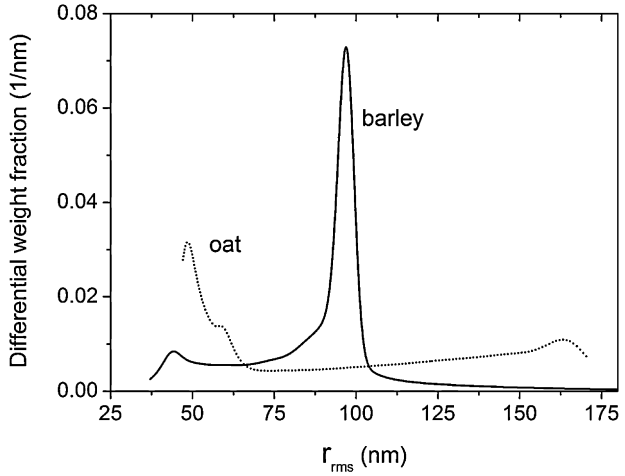

Fig. 3. Differential rms radius distribution for barley β-glucan (solid line) and oat β-glucan (dotted line).

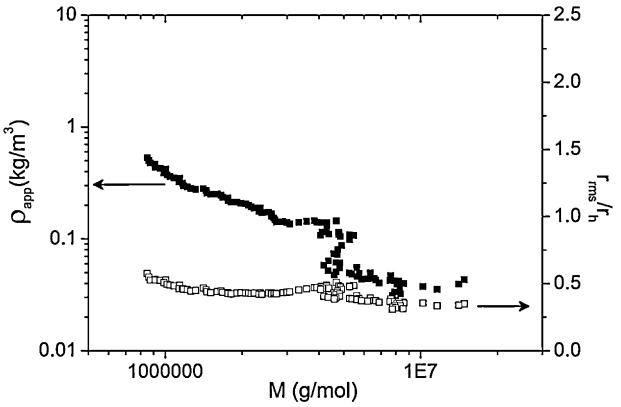

Fig. 4. Oat β-glucan apparent density (closed squares) and r_{rms}/r_h (open squares) vs. molar mass. Dissolution conditions: stirring in pure water; 70 °C, 20 min.

displays a "jump" at $4–5 \times 10^6$ g/mol which originates from insufficient mass resolution during separation for this subpopulation. The values for r_{rms}/r_h have only a very weak dependence on M and displays rather low values (typically what is expected for a swollen microgel structure) (Schmidt, Nerger, & Burchard, 1979). No values of r_{rms}/r_h corresponding to random coil (1.5–2.1) (Burchard, 1999) or rod-like conformation (1.7–3.0) (Coviello, Kajiwara, Burchard, Dentini, & Crescenzi, 1986; Wittgren, Borgström, Piculell, & Wahlund, 1998), as could be expected for molecularly dissolved β-glucan, can be observed. Barley β-glucan (Fig. 5) displays a stronger dependence of the apparent density on M. The apparent density initially decreases strongly with increasing $M/M_{w,0}$ and displays an inflection point at $M/M_{w,0} \approx 5–6$. This shows that in this $M/M_{w,0}$ interval the scaling of the sample components drastically change, which is also reflected in the plot of r_{rms}/r_h vs. $M/M_{w,0}$ (Fig. 5) which levels off to rather constant and low values. On the contrary to oat β-glucan, the barley β-glucan displays a variety of conformational properties (r_{rms}/r_h) over the investigated size range (Fig. 5). The lowest molar mass species appear more elongated and rod-like, followed by an intermediate size range where components appear to have a random coil conformation.

Barley β-glucan dissolved and analyzed in the FFF carrier liquid (10 mM $NaNO_3$) (I), 0.05 M NaOH (II) and 0.5 M NaOH (III), respectively, are shown in Fig. 6. The results show that dissolution in alkali was not sufficient to remove large species (assumed to be aggregates) in the samples. An interesting observation is that elution times are shorter in NaOH than in $NaNO_3$. It should also be

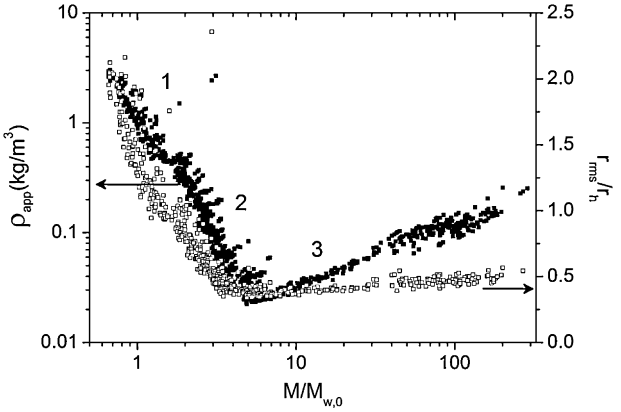

Fig. 5. Barley β-glucan apparent density (closed squares) and r_{rms}/r_h (open squares) vs. molar mass (M) normalized with weight-average molar mass of the barley beta-glucan single molecule ($M_{w,0}$) (as specified by the supplier). Dissolution conditions: stirring in pure water; 70 °C, 20 min.

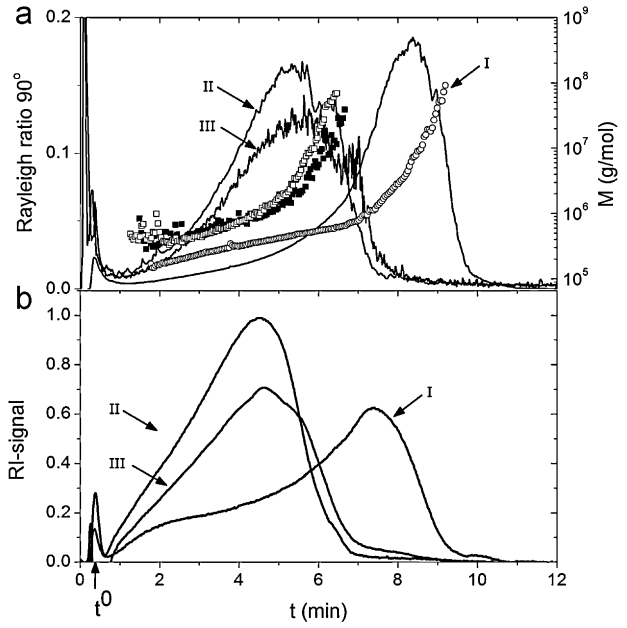

Fig. 6. Elution profiles for barley β-glucan dissolved and analyzed in aqueous NaOH and $NaNO_3$. (a) Rayleigh ratio at 90° scattering angle (solid lines) and molar mass (symbols); (I) 10 mM $NaNO_3$ (open circles), (II) 0.05 M NaOH (open squares), (III) 0.5 M NaOH (closed squares). (b) RI detector signal; (I) 10 mM $NaNO_3$, (II) 0.05 M NaOH, (III) 0.5 M NaOH.

remarked that fractionation appears to work satisfactory independent of NaOH concentration.

In Table 1 the results are summarized as averages and recoveries from the separation channel. The barley β-glucan average molar mass is rather unaffected by dissolution in alkali showing that the large species, assumed to be aggregates, are not dissociated by this treatment. In all cases the recoveries are high for barley β-glucan, with somewhat lower recoveries in NaOH which may indicate a slight degradation. For oat β-glucan the recovery is 87% which is somewhat low. Most likely, this is caused by low molar mass impurities in the sample as the void peak (unretained material) in the RI-detector was substantially higher (result not shown) for this sample compared to the barley β-glucan.

4. Discussion

Mild dissolution procedures result in wide molar mass and size distributions for the investigated β-glucans as has been observed previously (Ulmius et al., 2012). The results suggest that the β-glucans appear to have highly aggregated structures. The ratio between r_{rms} and r_h is a powerful characterization concept as it offers an insight into to conformational properties of the sample (Burchard, 1983, 1999). When used in conjunction with a fractionation technique it is possible to obtain conformational data over the entire size distribution and has been shown to be useful for the characterization of polysaccharides as for instance starch (Nilsson et al., 2006; Rojas, Wahlund, Bergenståhl, & Nilsson, 2008), glycogen (Fernandez et al., in press), exudate gums (Alftrén et al., 2012) and casein micelles (Glantz, Håkansson, Lindmark-Månsson, Paulsson, & Nilsson, 2010).

β-Glucan is a linear polysaccharide and is expected to behave as a chain with certain flexibility, depending on the persistence length (a). If the chain contour length (L) is sufficiently long in comparison to the persistence length, a random coil conformation is expected. Fig. 4 shows that no such conformations are present in the oat β-glucan. On the other hand, such structures (r_{rms}/r_h = 1.5–2.1 (Burchard, 1999)) are present in the barley β-glucan, at $M/M_{w,0} \approx 1$

Table 1
Averages of the different samples.

Sample	M_w (10^6 g/mol)	r_{rms} (nm)[a]	r_h (nm)[a]	Recovery (%)
Barley beta-glucan				
70 °C, 20 min	2.3	94	173	99
0.05 M NaOH	2.5	86	nd[b]	94
0.5 M NaOH	2.5	83	nd[b]	98
Oat beta-glucan				
70 °C, 20 min	3.3	141	282	87

[a] z-Average.
[b] Not determined.

(Fig. 5). The results for r_{rms}/r_h of the oat β-glucan sample, suggest that no or very little of the sample is molecularly dissolved. The results in Fig. 5 shows that the barley β-glucan displays drastically different scaling of objects over the molar mass distribution which can be divided in three domains (numbered 1–3 in Fig. 5).

In domain 1 the species show rod-like behaviour (i.e. $r_{rms}/r_h > 2.1$; $L < a$) and as chains become longer than a the conformation gradually changes to a random coil behaviour ($L > a$). For comparison, a (in water), for barley β-glucan, has been reported to be 83 nm (Grimm et al., 1995).

In domain 2 (Fig. 5) the apparent density decreases with increasing molar mass and r_{rms}/r_h = 0.5–1.5, suggesting that this domain consists of aggregated structures as r_{rms}/r_h = 1.2 corresponds to hyper branched structures (Burchard, 1999) and r_{rms}/r_h = 0.3–0.6 corresponding to swollen micro-gel structures (Burchard, 1999). Similar structures have been observed previously for poly(vinyl) acetate (Schmidt et al., 1979) as well as glycogen (Fernandez et al., in press). As the β-glucan is a linear chain such structures would not arise, was the β-glucan molecularly dissolved. The apparent density decrease with increasing molar mass in domain 2 which could be interpreted in terms of higher density for the smaller aggregates, however, care must be taken in interpreting apparent density for an interval of drastically changing conformation since it will be influenced by elongation to some extent.

In domain 3 (Fig. 5) an inflection point in the apparent density can be observed when a certain $M/M_{w,0}$ has been reached and a slight increase in apparent density is observed with increasing $M/M_{w,0}$. Furthermore, r_{rms}/r_h becomes rather independent on molar mass in this domain, showing that the species present correlate to highly swollen micro gel structures. The combination of apparent density and r_{rms}/r_h contradicts a growth of individual aggregate as such structures would be expected to decrease in apparent density with increasing size. Together these results suggest that domain 3 represents a higher level of aggregation consisting of secondary aggregates of primary aggregates (domain 2). Thus, we can estimate the primary aggregates to consist of roughly 6–8 individual β-glucan molecules (Fig. 5).

Based on the observations from the three domains in Fig. 5 it is then necessary to consider the structure of the β-glucan aggregates. Cereal β-glucans have been suggested to aggregate in micellar-like structures (Vårum, Smidsröd, & Brant, 1992). Furthermore, they have been suggested to aggregate in a fringed micelle structure in which the core of the aggregate is formed by the alignment of β-glucan chains, thus, resulting in a rather dense core with chains of the individual β-glucans protruding into the surrounding solution (Grimm et al., 1995). The fringed micelle structure is also supported by scanning probe micrographs (Wu et al., 2006). The trend of r_{rms}/r_h for barley β-glucan over the molar mass distribution in the current paper, agree with earlier findings for barley β-glucans investigated by batch light scattering (Grimm et al., 1995). However, the constant value of r_{rms}/r_h for large species was found to be around 1.0 but is lower in the current paper (Fig. 4 and domain 3, Fig. 5). A possible reason for this difference could be the differences in methods as Grimm et al. utilized batch static and dynamic light

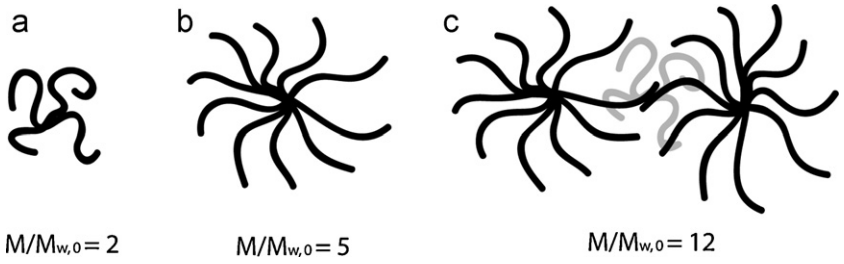

Fig. 7. Schematic illustration showing possible structures suggested, describing the results observed in Figs. 4–5. Supramolecular aggregates (a and b) and aggregated supramolecular aggregates (c) at different M/M_0.

scattering for their investigation. Hence, the results were based on average properties and as r_{rms} is a *z*-average, this would yield higher values for r_{rms}/r_h. From the description of the procedures in the paper by Grimm et al. it is, however, not possible to be conclusive on this point. The model of a dense aggregate core with chains protruding into the surrounding solution would explain the rather low values observed for r_{rms}/r_h in domain 2–3 (Fig. 5).

Fig. 7 shows schematic illustrations suggesting how the aggregate structure could evolve. At low degrees of aggregation (Fig. 7a) aggregates appear denser while for higher degrees of aggregation (Fig. 7b) the apparent density decreases as the chains would have less conformational freedom and, thus, would have to stretch somewhat in order to accommodate more chains in the aggregate. Similarly, this would result in a large hydrated perimeter of the aggregate reflected in the low values of r_{rms}/r_h. Fig. 7c shows a proposed structure of the secondary aggregates in which polydispersity of primary aggregates could give rise to the slight increase observed in the apparent density (Fig. 5, domain 3). It has previously been stated that the fringed micelle structure could not explain the gelation behaviour of cereal β-glucans (Li et al., 2011). However, our results suggest that aggregates of individual fringed micelles are present and could, thus, be involved in network formation.

It is interesting to note that the results in the current paper as well as those previously reported (Grimm et al., 1995; Wu et al., 2006) seem to suggest that aggregation occurs at specific locations in the macromolecular chain. A homogeneous aggregation would not be a likely explanation of the results observed as constant scaling of density with increasing size would be expected. This, in turn, raises questions regarding the underlying mechanism of aggregation and seems to rule out hydrogen bonding as a driving force for aggregation as it would be expected to occur at multiple sites in the β-glucan chain. The unlikely contribution of hydrogen bonding to glucan aggregation has recently been discussed elsewhere (Lindman, Karlström, & Stigsson, 2010). Rather it would be expected that the driving force for aggregation has other origins but any conclusions on this would, as of yet, be highly speculative.

In summary, the conformational and structural data in the current paper agrees with the fringed micelle structure of aggregates suggested previously (Grimm et al., 1995; Vårum et al., 1992; Wu et al., 2006). However, through utilization of the concept of apparent density over the size distribution the interpretation can be extended, suggesting the presence of aggregates of fringed micelles. It can also be concluded that the values of the apparent densities observed in the current paper are very low (<1 kg/m^3) compared to those observed for several other polysaccharides (Alftrén et al., 2012; Fernandez et al., in press; Nilsson et al., 2006; Rojas et al., 2008) again indicating swollen and micro gel-like structures.

Using NaOH (0.05 and 0.5 M) as dissolution and carrier liquid did neither remove the aggregates, nor reduce M_w in any significant manner. However, we observed a shift in the elution profiles to shorter elution times. At a NaOH concentration of 0.05 and 0.5 M, the pH will be about 12.7 and 13.7 respectively which will cause the β-glucans to become strongly charged and behave as polyelectrolytes (for glucose pK_a = 12.2–13.3) (Konopik & Leberl, 1949). This will have a large effect on the interaction between β-glucan molecules which will become strongly repulsive. The increased charge density in the molecules is likely to be the origin on the earlier elution. Several possible explanations exist for this behaviour. One possibility is that conformational changes occur, as an effect of the increased pH. However, no change in the scaling of r_{rms} vs. M could be observed (result not shown) making this an unlikely explanation. It could be expected that substantially increasing the charge density in the molecules, if not causing dissociation of aggregates, would lead to swelling and, thus, longer elution times (shorter distances to the accumulation wall in the separation channel). This would not explain the effects observed, and rather a slight increase in *z*-average r_{rms} is observed, which may be caused by slight dissociation of aggregates or degradation of molecules.

Another possibility is repulsion between sample species and the membrane surface. The membrane utilized (poly(ether) sulphone) has been shown to carry anionically charged groups (Artug & Hapke, 2006; Weis, Bird, & Nyström, 2003) which could give rise to repulsion between the membrane surface and sample components. However, the charge density for the membranes is rather low and the arising repulsion would be short ranged (high ionic strength) and could not explain the shift in repulsion as this would require more long ranged repulsion (in the order of a micrometer). A more likely explanation is that the thermodynamic force, which counteracts convective transport to the accumulation wall, is drastically increased when the sample species become highly charged and repulsion arise between sample components. This influences the sample concentration profile away from the accumulation wall and has rather long range effects (several μm) (Jönsson & Jönsson, 1996).

Finally, the membrane may also swell under the high pH conditions causing the channel height to decrease and, thus, giving rise to shorter elution times. As the retention time is proportional to the square of the channel height a decrease in channel height of about 30% compared to conditions with neutral pH would suffice to explain the observed shift in retention time (Wahlund & Giddings, 1987).

5. Conclusions

The results presented in this paper show that AsFlFFF-MALS-RI is a highly suitable technique for analyzing β-glucans and their aggregates. Important conformational properties are obtained over the entire size distribution and the results suggest that distinction between individual molecules, primary aggregates and secondary aggregates can be obtained. Oat β-glucan appeared to not be molecularly dissolved when samples were prepared in pure water while for barley β-glucan some of the material appeared molecularly dissolved. Furthermore, the results showed that alkaline conditions were not sufficient to dissociate barley β-glucan aggregates as has been suggested in previous studies.

Acknowledgements

The Swedish Research Council (VR), Stockholm, Sweden is acknowledged for financial support. Funding for instrumentation is gratefully acknowledged from: The Swedish Research Council for Environment, Agricultural Sciences and Spatial Planning (FORMAS), Stockholm, Sweden, The Royal Physiographic Society of Lund, Sweden and The Crafoord Foundation, Lund, Sweden.

References

Alftrén, J., Peñarrieta, J. M., Bergenståhl, B., & Nilsson, L. (2012). Comparison of molecular and emulsifying properties of gum arabic and mesquite gum using asymmetrical flow field-flow fractionation. *Food Hydrocolloids*, *26*(1), 54–62.

Andersson, M., Wittgren, B., & Wahlund, K. G. (2003). Accuracy in multiangle light scattering measurements for molar mass and radius estimations. Model calculations and experiments. *Analytical Chemistry*, *75*(16), 4279–4291.

Artug, G., & Hapke, J. (2006). Characterization of nanofiltration membranes by their morphology, charge and filtration performance parameters. *Desalination*, *200*, 178–180.

Beer, M. U., Wood, P. J., & Weisz, J. (1997). Molecular weight distribution and (1-3)(1-4)-β-D-glucan content of consecutive extracts of various oat and barley cultivars. *Cereal Chemistry*, *74*(4), 476–480.

Berry, G. C. (1966). Thermodynamic and conformatinal properties of polystyrene. I. Light-scattering studies on dilute solutions of linear polystyrenes. *Journal of Chemical Physics*, *44*(12), 4550–4564.

Burchard, W. (1983). Static and dynamic light scattering from branched polymers and bio-polymers. *Advances in Polymer Science*, *48*, 1–124.

Burchard, W. (1999). Solution properties of branched macromolecules. *Advances in Polymer Science*, *143*, 113–194.

Coviello, T., Kajiwara, K., Burchard, W., Dentini, M., & Crescenzi, V. (1986). Solution properties of xanthan. 1. Dynamic and static light scattering from native and modified xanthans in dilute solutions. *Macromolecules*, *1986*(19), 2826–2831.

Cui, W., Wood, P. J., Blackwell, B., & Nikiforuk, J. (2000). Physicochemical properties and structural characterization by two-dimensional NMR spectroscopy of wheat [beta]-D-glucan—Comparison with other cereal [beta]-D-glucans. *Carbohydrate Polymers*, *41*(3), 249–258.

Einstein, A. (1905). Uber die von der molekularkinatischen Theorie der Wärma geforderte Bewegung von in ruhenden Flussigkeiten suspendierten Teilchen. *Annalen der Physik*, *17*, 549–560.

European Food Safety Authority (2009). Scientific opinion on the substantiation of health claims related to beta-glucans and maintenance of normal blood cholesterol concentrations (ID 754, 755, 757, 801, 1465, 2934) and maintenance or achievement of a normal body weight (ID 820, 823) pursuant to Article 13(1) of Regulation (EC) No 1924/2006. *EFSA Journal*, *7*(9:1254).

European Food Safety Authority (2010). Scientific opinion on the substantiation of a health claim related to oat beta-glucan and lowering blood cholesterol and reduced risk of (coronary) heart disease pursuant to Article 14 of Regulation (EC) No 1924/2006. *EFSA Journal*, *8*(12:1885).

Fernandez, C., Rojas, C. C., & Nilsson, L. Size, structure and scaling relationships in glycogen from various sources investigated with asymmetrical flow field-flow fractionation and 1H-NMR. *International Journal of Biological Macromolecules*, doi:10.1016/j.ijbiomac.2011.05.016, in press.

Glantz, M., Håkansson, A., Lindmark-Månsson, H., Paulsson, M., & Nilsson, L. (2010). Revealing the size, conformation and shape of bovine casein micelles and aggregates with asymmetrical flow field-flow fractionation and multi-angle light scattering. *Langmuir*, *26*(15), 12585–12591.

Gómez, C., Navarro, A., Gamier, C., Horta, A., & Carbonell, J. V. (1997). Physical and structural properties of barley (1 → 3), (1 → 4)-β-D-glucan. Part III. Formation of aggregates analysed through its viscoelastic and flow behaviour. *Carbohydrate Polymers*, *34*(3), 141–148.

Grimm, A., Krüger, E., & Burchard, W. (1995). Solution properties of β-D-(1, 3)(1, 4)-glucan isolated from beer. *Carbohydrate Polymers*, *27*(3), 205–214.

Jönsson, A.-S., & Jönsson, B. (1996). Ultrafiltration of colloidal dispersions—A theoretical model of the concentration polarization phenomena. *Journal of Colloid and Interface Science*, *180*, 504–518.

Kivelä, R., Nyström, L., Salovaara, H., & Sontag-Strohm, T. (2009). Role of oxidative cleavage and acid hydrolysis of oat beta-glucan in modelled beverage conditions. *Journal of Cereal Science*, *50*(2), 190–197.

Konopik, N., & Leberl, O. (1949). Dissoziationskonstanten sehr schwacher Säuren. *Monatshefte fur Chemie*, *80*, 655–669.

Li, W., Cui, S. W., Wang, Q., & Yada, R. Y. (2011). Studies of aggregation behaviours of cereal β-glucans in dilute aqueous solutions by light scattering: Part I. Structure effects. *Food Hydrocolloids*, *25*(2), 189–195.

Li, W., Wang, Q., Cui, S. W., Huang, X., & Kakuda, Y. (2006). Elimination of aggregates of (1 → 3) (1 → 4)-beta-glucan in dilute solutions for light scattering and size exclusion chromatography study. *Food Hydrocolloids*, *20*(2–3), 361–368.

Lindman, B., Karlström, G., & Stigsson, L. (2010). On the mechanism of dissolution of cellulose. *Journal of Molecular Liquids*, *156*(1), 76–81.

Litzen, A. (1993). Separation speed, retention and dispersion is asymmetrical flow field-flow fractionation as functions of channel dimensions and flow-rates. *Analytical Chemistry*, *65*(4), 461–470.

Nilsson, L., Leeman, M., Wahlund, K. G., & Bergenståhl, B. (2006). Mechanical degradation and changes in conformation of hydrophobically modified starch. *Biomacromolecules*, *7*, 2671–2679.

Rojas, C. C., Wahlund, K.-G., Bergenståhl, B., & Nilsson, L. (2008). Macromolecular geometries determined with field-flow fractionation and their impact on the overlap concentration. *Biomacromolecules*, *9*, 1684–1690.

Schmidt, M., Nerger, D., & Burchard, W. (1979). Quasi-elastic light-scattering from branched polymers. 1. Polyvinylacetate and polyvinylacetate microgels prepared by emulsion polymerization. *Polymer*, *20*(5), 582–588.

Ulmius, M., Önning, G., & Nilsson, L. (2012). Solution behavior of cereal β-glucan as studied with asymmetrical flow field-flow fractionation. *Food Hydrocolloids*, *26*(1), 175–180.

US Food and Drug Administration. (1997). Food labeling: Health claims; soluble fiber from whole oats and risk of coronary heart disease. *Federal Register*, *62*, 15343–15344.

US Food and Drug Administration. (2008). Food labeling: Health claims; soluble fiber from certain foods and risk of coronary heart disease. *Federal Register*, *73*, 47828–47829.

Vårum, K. M., Smidsröd, O., & Brant, D. A. (1992). Light-scattering reveals micelle-like aggregation in the (1-3), (1-4)-beta-D-glucans from oat aleurone. *Food Hydrocolloids*, *5*(6), 497–511.

Wahlund, K. G., & Giddings, J. C. (1987). Properties of an asymmetrical flow field-flow fractionation channel having one permeable wall. *Analytical Chemistry*, *59*(9), 1332–1339.

Weis, A., Bird, M. R., & Nyström, M. (2003). The chemical cleaning of polymeric UF membranes fouled with spent sulphite liquor over multiple operational cycles. *Journal of Membrane Science*, *216*, 67–79.

Wittgren, B., Borgström, J., Piculell, L., & Wahlund, K. G. (1998). Conformational change and aggregation of kappa-Carrageenan studied by flow field-flow fractionation and multi angle light scattering. *Biopolymers*, *45*, 85–96.

Wu, J., Zhang, Y., Wang, L., Xie, B. J., Wang, H. B., & Deng, S. P. (2006). Visualization of single and aggregated hulless oat (*Avena nuda* L.) (1 → 3), (1 → 4)-beta-D-glucan molecules by atomic force microscopy and confocal scanning laser microscopy. *Journal of Agricultural and Food Chemistry*, *54*(3), 925–934.